AD A057 765

TECHNICAL REPORT ARLCB-TR-78004

FATIGUE-CRACK PROPAGATION THROUGH A MEASURED RESIDUAL STRESS FIELD IN ALLOY STEEL

J. H. Underwood
L. P. Pook
J. K. Sharples

TECHNICAL LIBRARY

February 1978

US ARMY ARMAMENT RESEARCH AND DEVELOPMENT COMMAND
LARGE CALIBER WEAPON SYSTEMS LABORATORY
BENÉT WEAPONS LABORATORY
WATERVLIET, N. Y. 12189

AMCMS No. 36525000204

DA Project No. 579101900GR1

PRON No. GG-8-25791-GG-M7

APPROVED FOR PUBLIC RELEASE; DISTRIBUTION UNLIMITED

DISCLAIMER

The findings in this report are not to be construed as an official Department of the Army position unless so designated by other authorized documents.

The use of trade name(s) and/or manufacturer(s) does not constitute an official indorsement or approval.

DISPOSITION

Destroy this report when it is no longer needed. Do not return it to the originator.

SECURITY CLASSIFICATION OF THIS PAGE *(When Data Entered)*

REPORT DOCUMENTATION PAGE

READ INSTRUCTIONS BEFORE COMPLETING FORM

1. REPORT NUMBER: ARLCB-TR-78004
2. GOVT ACCESSION NO.:
3. RECIPIENT'S CATALOG NUMBER:

4. TITLE *(and Subtitle)*: FATIGUE-CRACK PROPAGATION THROUGH A MEASURED STRESS FIELD IN ALLOY STEEL

5. TYPE OF REPORT & PERIOD COVERED:

6. PERFORMING ORG. REPORT NUMBER:

7. AUTHOR(s):
J. H. Underwood
L. P. Pook
J. K. Sharples

8. CONTRACT OR GRANT NUMBER(s):

9. PERFORMING ORGANIZATION NAME AND ADDRESS:
Benet Weapons Laboratory
Watervliet Arsenal, Watervliet, N.Y. 12189
DRDAR-LCB-TL

10. PROGRAM ELEMENT, PROJECT, TASK AREA & WORK UNIT NUMBERS:
AMCMS No. 36525000204
DA Proj. No. 579101900GR1
PRON No. GG-8-25791-GG-M7

11. CONTROLLING OFFICE NAME AND ADDRESS:
US Army Armament Research and Development Command
Large Caliber Weapon Systems Laboratory
Dover, New Jersey 07801

12. REPORT DATE: February 1978

13. NUMBER OF PAGES: 17

14. MONITORING AGENCY NAME & ADDRESS *(if different from Controlling Office)*:

15. SECURITY CLASS. *(of this report)*: UNCLASSIFIED

15a. DECLASSIFICATION/DOWNGRADING SCHEDULE:

16. DISTRIBUTION STATEMENT *(of this Report)*

Approved for public release; distribution unlimited.

17. DISTRIBUTION STATEMENT *(of the abstract entered in Block 20, if different from Report)*

18. SUPPLEMENTARY NOTES

19. KEY WORDS *(Continue on reverse side if necessary and identify by block number)*
Crack Propagation
Fracture (materials)
Alloys

20. ABSTRACT *(Continue on reverse side if necessary and identify by block number)*

Fatigue crack-propagation tests were performed using 5 by 30mm cross-section bend specimens of a nickel-chromium-molybdenum steel. The fatigue crack-propagation rate was determined from a group of stress-free specimens by measuring crack length on the specimen surfaces at intervals during cycling. Residual stress was produced in a second group of specimens by using a localized plastic deformation process. Resistance strain gages were first applied

(continued on reverse side)

DD FORM 1 JAN 73 1473 EDITION OF 1 NOV 65 IS OBSOLETE

SECURITY CLASSIFICATION OF THIS PAGE *(When Data Entered)*

Continued from Block 20.

near one edge of each specimen along the line of intended crack growth. A series of 1mm deep plastic indentations was then made along the opposite edge of the specimen using a 25mm diameter pin. The strain gages provided a direct, accurate measure of the elastic, residual stress produced on one side of the specimen due to the local plastic deformation on the opposite side.

Measured crack-propagation rates in the specimens with residual stress are compared with rates in residual stress-free specimens. Crack-propagation rates are lower, as expected, near the edge of the specimen where the initial residual stress is compressive. Propagation rates remain lower even as the crack grows deeper into the specimen where the initial residual stress is tensile, which is not what would be expected from a simple superposition of stresses. However, an analysis involving the combination of the applied stress-intensity factor with that estimated from a redistribution of the residual stress in the specimens can account for the lower crack-propagation rates.

Authorized Reprint from
Special Technical Publication 631
Copyright
American Society for Testing and Materials
1916 Race Street, Philadelphia, Pa. 19103
1977

J. H. Underwood,[1] *L. P. Pook,*[2] *and J. K. Sharples*[2]

Fatigue-Crack Propagation Through a Measured Residual Stress Field in Alloy Steel

REFERENCE: Underwood, J. H., Pook. L. P., and Sharples, J. K., **"Fatigue-Crack Propagation Through a Measured Residual Stress Field in Alloy Steel,"** *Flaw Growth and Fracture, ASTM STP 631,* American Society for Testing and Materials, 1977, pp. 402–415.

ABSTRACT: Fatigue crack-propagation tests were performed using 5 by 30 mm cross-section bend specimens of a nickel-chromium-molybdenum steel. The fatigue crack-propagation rate was determined from a group of stress-free specimens by measuring crack length on the specimen surfaces at intervals during cycling. Residual stress was produced in a second group of specimens by using a localized plastic deformation process. Resistance strain gages were first applied near one edge of each specimen along the line of intended crack growth. A series of 1-mm-deep plastic indentations was then made along the opposite edge of the specimen using a 25-mm-diameter pin. The strain gages provided a direct, accurate measure of the elastic, residual stress produced on one side of the specimen due to the local plastic deformation on the opposite side.

Measured crack-propagation rates in the specimens with residual stress are compared with rates in residual stress-free specimens. Crack-propagation rates are lower, as expected, near the edge of the specimen where the initial residual stress is compressive. Propagation rates remain lower even as the crack grows deeper into the specimen where the initial residual stress is tensile, which is not what would be expected from a simple superposition of stresses. However, an analysis involving the combination of the applied stress-intensity factor with that estimated from a redistribution of the residual stress in the specimens can account for the lower crack-propagation rates.

KEY WORDS: crack propagation, fracture (materials), alloys

Nomenclature

- a Crack depth
- B Specimen thickness

[1]Research engineer, Materials Engineering Division, U.S. Army, Benet Weapons Laboratory, Watervliet, N.Y. 12189.

[2]Principal scientific officer and higher scientific officer, respectively, National Engineering Laboratory, East Kilbride, Glasgow, Scotland.

K_I Opening mode stress-intensity factor
K_{max} K_I at maximum load in fatigue cycle
K_{min} K_I at minimum load in fatigue cycle
K_a K_I corresponding to the amplitude of alternating load in fatigue cycle
K_R K_I corresponding to the residual stress distribution at maximum load in fatigue cycle
K_{op} K_I corresponding to the residual stress distribution at minimum load in fatigue cycle
ΔK Range of K_I in fatigue cycle
ΔK_R Range of K_I in fatigue cycle including effect of residual stress
N Number of fatigue cycles
P_a Amplitude of alternating load in fatigue cycle
P_m Mean load in fatigue cycle
W Specimen depth
y Distance from notched edge of specimen
y_o y at the point of zero residual stress
σ_R Residual stress at $y = 0$
$\sigma_R{}^1$ Bending component of residual stress at $y = 0$
$\sigma_{R\text{-ave}}$ Average residual stress over the range $a/2 < y < 3a/2$

Fatigue-crack propagation in metal samples which contain residual stress is a subject of considerable interest. In most cases, however, the distribution and magnitude of residual stress are not known with much certainty. The uncertainty is caused by the fact that the processes which produce residual stress in a specimen, such as plastic deformation, thermal treatment, and metallurgical phase change, nearly always preclude an accurate calculation or measurement of residual stress. Linear-elastic analyses seldom can be used directly to determine the residual stress which results from these processes because they involve nonlinear deformations.

Even if the residual stress present in a sample were known with certainty, its effect on the fatigue crack-propagation rate would be difficult to assess. Methods for including the effect of residual stress in fracture mechanics descriptions of fatigue crack-propagation rate are not at all well developed. The approach often taken is simply adding the residual stress to the applied stress on the sample and using such a modified stress to calculate K_I, which is then used to describe the fatigue crack-propagation rate in the usual manner. This approach seems correct for sufficiently shallow cracks, that is, for crack depths which are small relative to sample dimensions and relative to the depth of the residual stress distribution. For other than shallow cracks, and most real situations are in this category, the addition of stress approach is merely an estimate of unknown accuracy, because the presence of the crack may cause a basic change in the residual stress distribution.

Based on the foregoing rationale, we planned a series of experiments in which the effect of an accurately measured residual stress on fatigue crack-propagation rate could be measured, and we planned to use the results to indicate an improved approach for including residual stress effects in a fracture-mechanics description of crack-propagation rate. The specific objectives of the work are (*a*) to produce a residual stress distribution in specimens of a high-strength steel and obtain an accurate measurement of the distribution, (*b*) measure fatigue crack-growth rate in the specimens and in stress-free comparison specimens, and (*c*) describe the crack-propagation rate using a superposition of applied stress intensity and the stress intensity determined from the residual stress distribution.

Test Procedures

Specimens

Ten specimens were machined from a single piece of forged steel of the following composition: 0.35C, 3.4Ni, 1.8Cr, 0.6Mo, 0.5Mn, 0.1V. The yield strength, tensile strength, and fracture toughness of the steel are 1210 MN/m^2, 1370 MN/m^2, 145 $MN/m^{3/2}$, respectively. The specimens were made to the following dimensions: thickness, B, 5.1 mm, depth, W, 30.0 mm, and length, 200 mm. A 0.3-mm-deep notch with a 0.05-mm root radius was cut across the thickness of each specimen at midlength. A photo of the center portion of one of the specimens is shown as Fig. 1.

Producing the Residual Stress

Residual stress was produced in six of the test specimens by using a

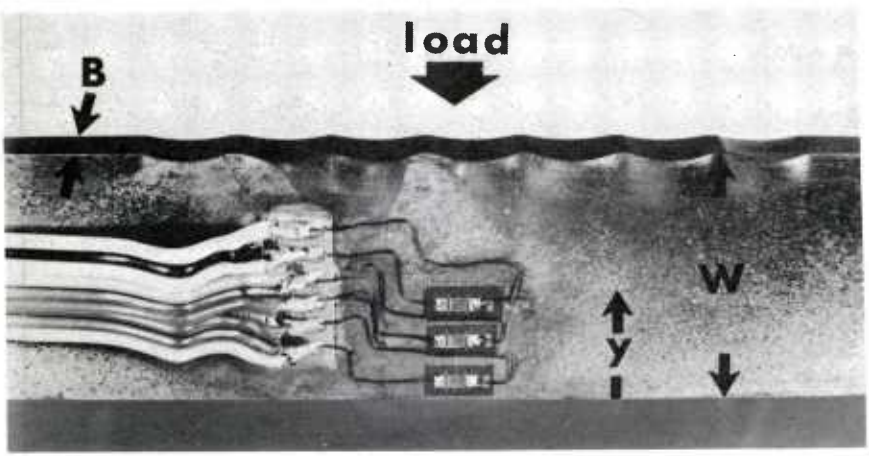

FIG. 1—*Photograph of specimen.*

localized plastic deformation process. Resistance strain gages were first applied to both sides of the specimen along the line of intended fatigue-crack growth. In general, three gages were applied to each side in the area near the notched edge of the specimen (see Fig. 1). A series of 1-mm deep, 5-mm long plastic indentations were then made along the opposite edge of the specimen using a 25-mm diameter pin mounted in a universal testing machine. The plastic indentations can be visualized as roughly equivalent to a series of wedges driven into the edge of the specimen. The strain gages provide a direct, accurate measurement of the elastic residual stress produced near one edge of the specimen due to the local plastic deformation along the opposite edge. The plastic deformation appeared to extend inward from the edge about 4 mm, while the strain gages were placed 15 to 30 mm from the deformed edge. So we are quite sure that no direct effect of the plastic deformation is recorded by the gages but only the induced elastic, residual deformation of the specimen.

The measured residual stress data are shown in Fig. 2. Each point represents the average strain from two gages on opposite sides which has been converted to a stress value using the elastic modulus. The data are well represented by the straight line shown, with the exception of the data from specimen T-5 which can be represented by a quite similar line. We attribute the difference for T-5 to a higher indentation load for this specimen.

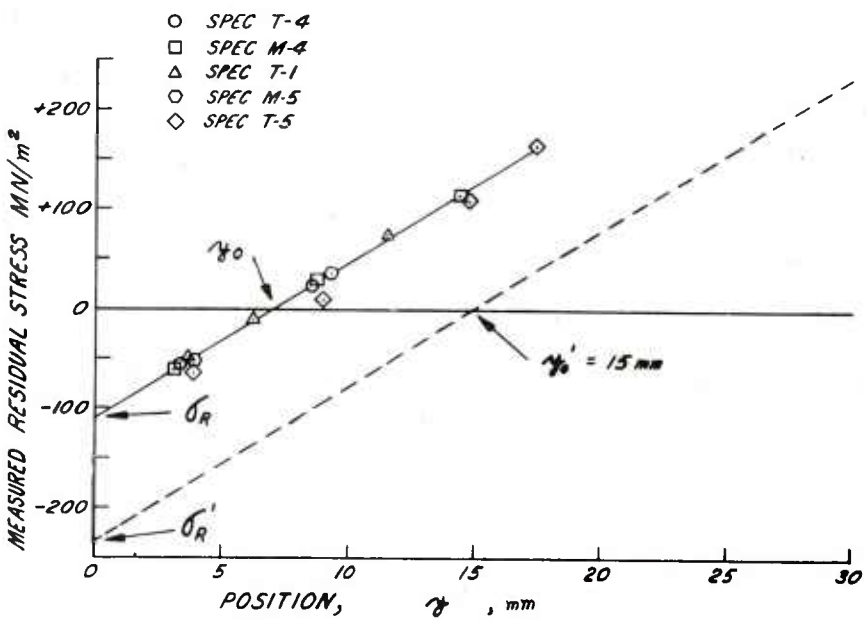

FIG. 2—*Measured residual stress distribution.*

The measured residual stress distribution is quite linear to beyond the specimen midpoint, $y/W = 0.5$. Then, the stress must drop sharply at some point, possibly at $y/W = 0.8$, pass through zero a second time, and approach a negative value about equal to the yield strength at the deformed edge, $y/W = 1.0$. A stress distribution of this sort meets the basic requirements that forces and moments be in balance. Balance of forces requires that the total area above and below the zero stress line be equal. Balance of moments requires that there be at least three separate areas above and below the zero stress line, because it is easy to show that two equal areas with one above and one below the zero stress line will always produce an unbalanced moment.

The actual stress distribution as just discussed would be difficult to include in a fracture-mechanics analysis. In the analysis used here, we assume that the residual stress distribution remains linear across the full width of the specimen. While this is not true, it may be a good approximation for describing the effect of residual stress on fatigue crack growth rate up to the specimen midpoint. In addition, a linear residual stress distribution can be represented exactly by the superposition of two familiar stress distributions; namely, a pure bending stress distribution shown as the dashed line in Fig. 2, and a uniform tension stress distribution which represents the difference between the two lines in Fig. 2. Further details will be discussed later.

Fatigue Tests

The fatigue crack-propagation tests were performed in three-point bending using a lower support span of 120 mm. The upper load point was centered on the span and directly over the strain gage and notch location (see Fig. 1). The load was applied to the specimen, and the specimen was supported by means of the blunt knife edges with a tip radius of about 1.0 mm which were supplied with the fatigue testing machine used for the tests. An electromagnetic fatigue machine was used, operating at 130 Hz at room temperature. The test conditions are listed in Table 1, including the alternating and mean loads and the measured residual stress information for each specimen. For three of the specimens containing residual stress, the notch was deepened much beyond the initial 0.3 mm depth. This caused a significant change in the fatigue crack-propagation rate for equivalent total notch plus crack depths as shown later.

The crack length was measured at intervals during the test on both sides of the specimen using a seven power microscope. For most of the data, the crack length readings from the two sides varied by less than 0.5 mm. The average values were plotted against number of cycles, a smooth curve was drawn through the points, and the slope of the curve was measured at intervals. We make no apology for this manual procedure. When it is

TABLE 1—*Test conditions.*

Specimen Number	Alternating Load, P_a, kN	Mean Load, P_m, kN	Residual Stress at $y = 0$, σ_R, MN/m^2	Position at zero residual stress, y_0, mm	Notch Depth, mm
			Stress Free		
M-1	1.25	1.50	0	...	0.3
M-6	2.50	3.00	0	...	0.3
T-2	2.50	3.00	0	...	0.3
T-6	3.50	4.20	0	...	0.3
			Residual Stress		
T-4	1.25	1.50	−108	7.1	0.3
M-4	2.00	2.40	−108	7.1	0.3
T-3	3.50	4.20	−108	7.1	0.3
			Residual Stress With Deep Notch		
T-1	1.50	1.70	−108	7.1	7.9
M-5	1.75	2.10	−108	7.1	5.0
T-5	2.50	3.00	−124	8.0	4.6

done properly, the results are every bit as reliable as those using computer aided methods. Plots of crack length, a, against number of cycles, N, are shown in Fig. 3 for six of the specimens tested. The zero point for N is arbitrary, since the concern here is with da/dN for a given crack length, loading, and residual stress condition.

Test Results and Analysis

Stress-Free Specimens

Crack-propagation tests were performed with the stress-free specimens to obtain results with which to compare the results from specimens containing residual stress. The a versus N data are shown in Fig. 3, including two specimens tested at the same load. The good agreement between the two repeat specimens is apparent in the a versus N plot and in the log ΔK versus da/dN plot shown in Fig. 4*a*. The straight line, upper bound to the growth-rate data in Fig. 4*a*, is typical of this material [*1*].[3] The deviations from the straight line are larger than we would expect for tests of this type, and the deviations appear to be systematic with a/W, as can be seen by the values of a/W shown in Fig. 4*a* which correspond to the beginning, middle, and end of the tests. For a/W values above 0.3 the deviations from the straight line become significant, as indicated by the dashed lines.

[3] The italic numbers in brackets refer to the list of references appended to this paper.

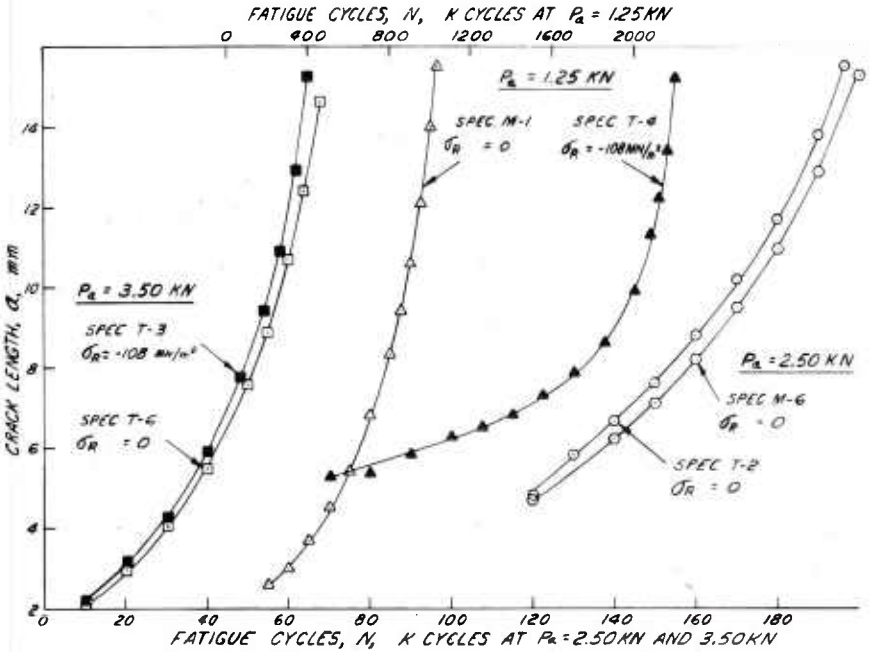

FIG. 3—*Measured crack length versus number of cycles.*

Crack Length Effect on da/dN

The deviations from the straight line in the data of Fig. 4*a* can be well represented by using the following modified ΔK function in the log ΔK versus log da/dN plot

$$\Delta K_{\text{mod}} = (1 - [a/W]^2)\Delta K \tag{1}$$

The ΔK values are calculated in the usual manner using the K relations from Ref *2*. When the modified ΔK expression is used to plot the results from the stress-free specimens, the data are all close to the expected straight line relation (see Fig. 4*b*). This result led us to the conclusion that for our tests there is a crack length effect on da/dN which is independent of the variation of ΔK with crack length.

The form of Eq 1 was chosen arbitrarily to fit the data. But Eq 1 also could be a representation of a crack-closure effect as proposed by Elber [*3*]. Crack length is one of the variables suggested by Elber with potential effect on crack-propagation rate through crack closure. And although crack length was not a significant variable in Elber's tension-fatigue tests with

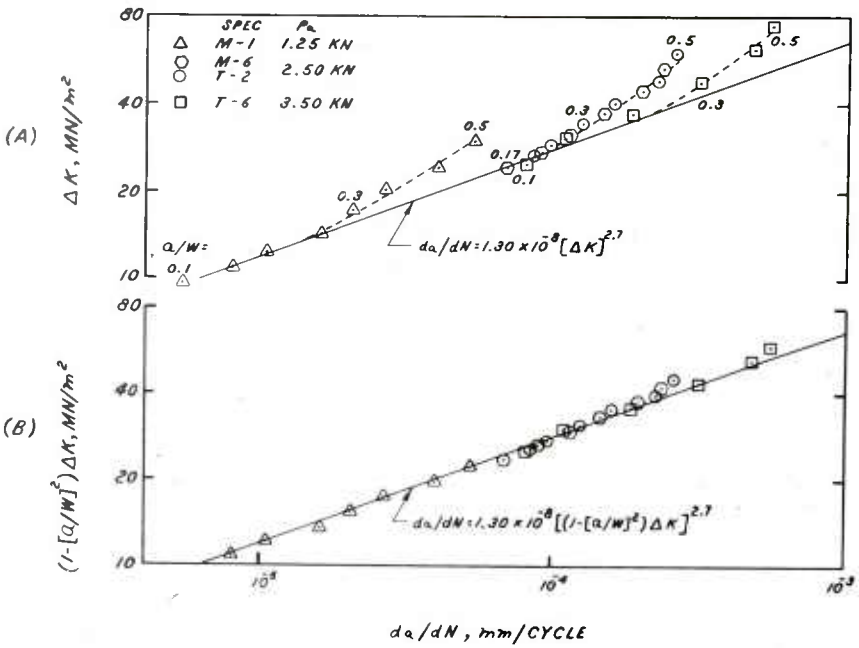

FIG. 4—ΔK *versus growth rate for stress free specimens*; (a) *conventional* ΔK *and* (b) *modified* ΔK *function.*

an aluminum alloy, the bend tests with a steel alloy in this work could be affected by crack length. Alternatively, Eq 1 could be a representation of an R-curve effect in fatigue-crack propagation. Pook and Greenan [*4*] have suggested that the resistance to fatigue-crack growth can increase with the amount of crack growth in a similar manner to the R-curve effect observed in monotonic loading of thin plate and sheet. Finally, a suggestion by an anonymous reviewer of this paper is that the deviation from the straight line in Fig. 4*a* for large a/W could be the result of an axial restraint applied to the specimen due to the friction at the specimen supports. Particularly, as the rotation of the specimen halves becomes significant at large a/W, the friction between the fixed specimen supports and the specimen could limit the rotation and cause a reduction in the value of K at maximum load and, thus, a reduction in the ΔK applied to the specimen.

It is not our intention here to relate the crack-length effect on da/dN to any particular process or model. It is only necessary to describe the crack-length effect so that it can be separated from the effect of residual stress on fatigue crack-propagation rate, the main topic of interest. So the modified ΔK function is used in the subsequent plots of ΔK versus da/dN.

Specimens Containing Residual Stress

The results from crack-propagation tests in three specimens containing residual stress and with a 0.3-mm notch are shown in Fig. 5. Results from similar specimens, but with much deeper notches of about 5 mm, are shown in Fig. 6. The data are plotted using the modified ΔK function, and

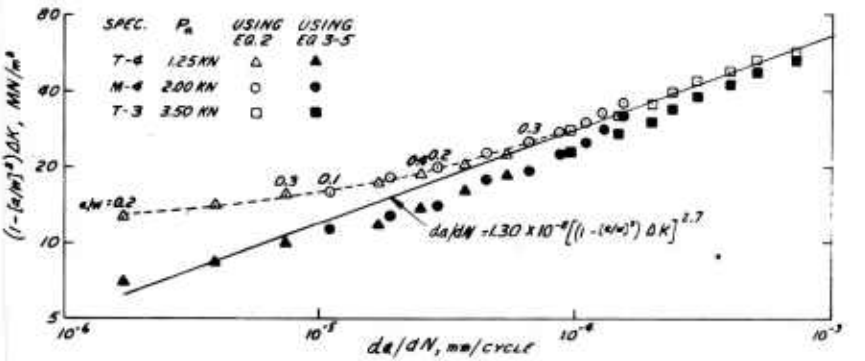

FIG. 5—*Modified* ΔK *function versus growth rate for specimens with residual stress and a shallow notch.*

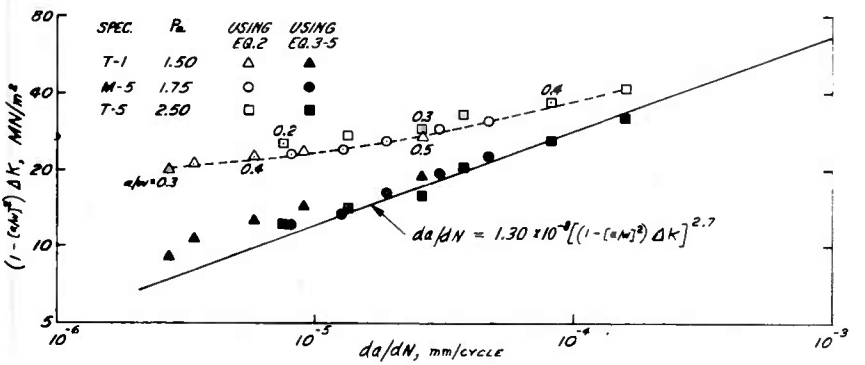

FIG. 6—*Modified* ΔK *function versus growth rate for specimens with residual stress and a deep notch.*

the straight line shown is the line which represents the stress-free results in Fig. 4. The ΔK values are calculated in two ways in Figs. 5 and 6. One is the conventional method. With the mean load positive and larger than the alternating load, and if the effect of residual stress is ignored, then ΔK has the straightforward definition

$$\Delta K = 2K_a \text{ for } P_m > P_a,\ \sigma_R = 0 \tag{2}$$

where K_a is the K_I value which corresponds to the alternating load on the specimen.

The second method for calculating ΔK includes an attempt to account for the effect of residual stress and is outlined as follows

$$\Delta K_R = (K_{max} + K_R) - (K_{min} + K_{op}) \quad (3)$$

where ΔK_R is the ΔK including the effects of residual stress, K_{max} and K_{min} have the usual definitions of the maximum and minimum K_I applied during the fatigue cycle, K_R is the K_I value which simulates the effect of the residual stress at the point of maximum load during the fatigue cycle, and K_{op} is the K_I value which simulates the effect of residual stress at the point of minimum load during the cycle. The approach used here is patterned after the Elber [*3*] model, but the situation is somewhat different. In the tests here, the amount of crack-tip plastic deformation, as measured by the ratio of ΔK to yield strength, is very much lower than in Elber's tests. Still, crack closure is believed to have occurred in the tests here but due to presence of residual stress rather than crack-tip plastic deformation. The first term in Eq 3 represents the reduction in the amount of crack opening at maximum load due to the presence of residual stress, and the second term represents the delayed opening of the crack at some point in the cycle above minimum load due to the presence of residual stress.

Redistribution of Residual Stress

The procedure for determining values for K_R and K_{op} in Eq 3 is discussed in relation to the sketches in Fig. 7. Shown here are the redistributed residual-stress gradients that we expect at maximum and minimum loads in specimens with very short and very long notches. The sketches depict the situation in which the total length of notch plus crack is in the same order of size as y_0, which is the situation for much of the test data presented here.

In Fig. 7, and the related discussions, we describe how the original residual stress distribution in the specimens as shown in Fig. 2 could become shifted or redistributed due to the combined effect of the notch plus crack arrangement and the load condition of the specimen.

Referring to Fig. 7 (*a* and *b*), we expect that a redistribution of residual stress has occurred at maximum load in the fatigue cycle and that the final redistributed stress is the same for specimens which are predominantly notched or cracked. At maximum load neither the now opened crack nor the notch can support any residual stress, but neither can they relieve any residual stress because the source of the residual stress is on the opposite side of the specimen. So as an estimate, we expect that the residual-stress distribution formally present with no crack or notch is still present but is

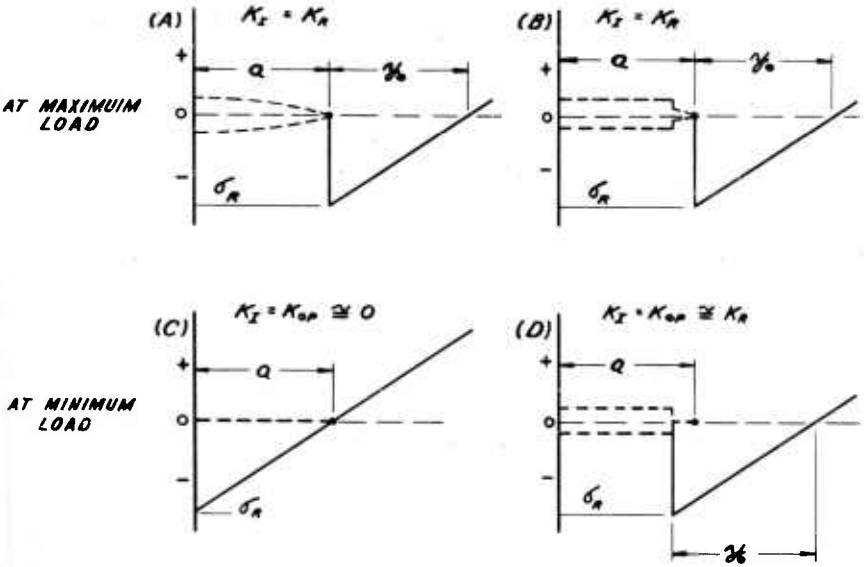

FIG. 7—*Expected residual stress distribution for various test conditions.*

shifted ahead to the crack tip as shown in Fig. 7 (*a* and *b*). And the K_I which corresponds to the shifted residual-stress distribution is the K_R in Eq 3.

Referring to Fig. 7*c*, at minimum load in the fatigue cycle in a cracked specimen, we expect that the residual stress distribution is unchanged from the uncracked situation because the crack has no effect on the compressive residual stress. And for this same reason there is no K_I in this situation.

Referring to Fig. 7*d*, at minimum load in a specimen which is predominantly notched, we expect that the stress distribution is shifted to the tip of the notch; the K_I which corresponds to this shifted stress distribution is the K_{op} in Eq 3 and, in addition, is approximately equal to K_R. This is a reasonable estimate in the limit as the crack ahead of the notch becomes very small, and it may remain a useful estimate for most of the test results here.

If the rationale discussed in relation to Fig. 7 is accepted, then Eq 3 can be rewritten as follows

$$\Delta K_R = 2K_a + K_R \quad \text{for cracked specimens}$$
$$\Delta K_R = 2K_a + 2K_R \quad \text{for notched specimens} \tag{4}$$

For a cracked specimen with a negligibly small notch, Eq 4 describes the reduction in ΔK caused by the addition of a negative K_I due to the residual stress. For a notched specimen with a small crack ahead, Eq 4 describes a

larger reduction in K, because the negative K_I due to the residual stress can affect the applied K_I at low applied loads as well as high.

In order to determine ΔK_R from Eq 4, an expression for K_R is needed. Since the stress distribution in Fig. 7 which is to be represented by K_R is a discontinuous distribution and is only an estimate, then a simple expression for K_R is called for and is given as follows

$$K_R = \sigma_{R\text{-ave}}(\pi a)^{1/2} \tag{5}$$

where $\sigma_{R\text{-ave}}$ is the average value of the redistributed residual stress near the crack tip, that is, over the range $a/2 < y < 3a/2$. Values of K_R calculated from Eq 5 assuming a shifted residual-stress distribution as indicated in Fig. 7 and using $\sigma_R = -108$ MN/m^2 are listed in Table 2. Also listed

TABLE 2—*Values of* K_R, *the* K_I *which simulates residual stress.*

a, mm	a/W	K_R from Eq 5 with redistribution MN/m$^{3/2}$	K_R from Eq 6 no redistribution MN/m$^{3/2}$
3	0.1	−4.7	−11.3
6	0.2	−5.9	−14.5
9	0.3	−6.3	−18.2
12	0.4	−6.0	−22.5
15	0.5	−5.5	−27.2

are values from the following expression for K_R based on the assumption that the residual-stress distribution remains unchanged during fatigue crack growth

$$(K_R)_{a\to 0} = 1/6\ \sigma_R{}'\, Y_B(a)^{1/2} + (\sigma_R{}' - \sigma_R)\ Y_T(a)^{1/2} \tag{6}$$

In Eq 6, $\sigma_R{}'$ is the outer fiber stress due to the pure bending component of the residual stress distribution (see Fig. 2), and Y_B and Y_T are the dimensionless K_I factors for pure bending and uniform tension [*2,5*]. Because of the assumption of a residual-stress distribution which does not redistribute with crack growth, Eq 6 is expected to be most appropriate for small values of a. Equation 6 describes a superposition of the K_I from the pure bending component of the residual-stress distribution and the K_I from the uniform tension component of the distribution (see Fig. 2). Together, these simulate the K_I which would be produced by the linear portion of the measured residual-stress distribution. It would be tempting to use Eq 6 to represent K_R since it is a bit more elegant. But it does not include the effect of redistribution of residual stress, and, as will be discussed shortly, it is not supported by the test results.

Results with Redistribution of Residual Stress

Returning to the discussion of Figs. 5 and 6, the data plotted using Eq 2, which is the conventional method for determining ΔK, result in da/dN values at low-ΔK which are lower, by up to a factor of 10, than those from stress-free specimens represented by the straight line. Further, it is interesting to note that the da/dN values remain significantly lower even at crack depths beyond $a/W = 0.3$. Considering that the residual stress at points beyond $a/W = 0.24$ in the uncracked specimen was a tensile stress, a simple superposition of stress would predict a higher da/dN. When the data are plotted using the method indicated by Eqs 3 through 5 which includes the effect of residual stress and a redistribution of residual stress, then the da/dN values are in reasonable agreement with the stress-free results. If the effect of residual stress were included but without the assumption of redistribution of stress, that is, using Eq 6, the result would not make sense. In fact, if the Eq 6 values are used to calculate ΔK, negative ΔK values result in some cases.

One further point regarding the results in Figs. 5 and 6 should be discussed. The data plotted using the conventional method give a clear indication that the effect of residual stress is independent of crack depth. Adjacent points on the smooth curve through the data often correspond to crack depths which differ by a factor of two to three, as indicated by the a/W values shown for selected data points. We view this crack depth independence as further support for the residual-stress-redistribution model used to interpret the results. Crack depth independence of K_I associated with the residual stress can be visualized if the stress distribution is considered as a local closing effect on the crack tip which occurs over an area which is small relative to crack length. For relatively deep cracks, this may be close to correct. It is interesting, although perhaps fortuitous, that the residual-stress redistribution approach of Eq 5 produces a K_I which is relatively independent of crack length for deep cracks (see Table 2).

Closing

The nature of the results obtained in the tests here and the relevancy of the analysis used to interpret the results are both highly dependent on the process which was used to produce the residual stress. In the process used here, the plastic deformation which caused the residual stress was remote from the area of fatigue cracking. A remote source of residual stress is a basic requirement for the redistribution model discussed here. A plastic deformation process can be conceived which would produce a similar initial residual-stress distribution, as that measured in the specimens here, but which would include plastic deformation in the area of subsequent fatigue cracking. Then, as the crack grows through the area of plastic

deformation, which is also the source of the residual stress, a combination of relief of residual stress and redistribution of residual stress will occur. The effect on the crack-growth rate could be quite different than that in the specimens here with a remote source of residual stress.

Although a rigorous analysis has not been possible in this work, the results obtained demonstrate that the behavior of fatigue cracks in residual stress fields can be described using fracture-mechanics methods. Further progress will depend at least as much on obtaining a fuller understanding of the applied mechanics of situations of interest, as on the accumulation of further experimental data. Of central importance will be the determination of the nature of residual stress redistribution in loaded, cracked bodies.

Acknowledgments

The authors are happy to acknowledge the help of J. A. Mackinnon of the National Engineering Laboratory for his help in planning and conducting the experiments described here.

Mr. Underwood acknowledges the support of the Secretary of the U.S. Army Research and Study Fellowship program which sponsored this work.

References

[1] Frost, N. E., Marsh, K. J., and Pook, L. P., *Metal Fatigue,* Claredon Press, Oxford, 1974.

[2] Srawley, J. E. and Gross, B., *Engineering Fracture Mechanics,* Vol. 4, 1972, pp. 587–589.

[3] Elber, Wolf in *Damage Tolerance in Aircraft Structures, ASTM STP 486,* American Society for Testing and Materials, 1971, pp. 230–242.

[4] Pook, L. P. and Grennan, A. F., "Various Aspects of the Fatigue Crack Growth Threshold in Mild Steel," presented at Conference on Fatigue Testing and Design, City University, London, England, April 1976, Society of Environmental Engineers Fatigue Group.

[5] Brown, W. F. and Srawley, J. E., *Plane Strain Crack Toughness Testing of High Strength Metallic Materials, ASTM STP 410,* American Society for Testing and Materials, 1966.

WATERVLIET ARSENAL INTERNAL DISTRIBUTION LIST

May 1976

	No. of Copies
COMMANDER	1
DIRECTOR, BENET WEAPONS LABORATORY	1
DIRECTOR, DEVELOPMENT ENGINEERING DIRECTORATE	1
ATTN: RD-AT	1
RD-MR	1
RD-PE	1
RD-RM	1
RD-SE	1
RD-SP	1
DIRECTOR, ENGINEERING SUPPORT DIRECTORATE	1
DIRECTOR, RESEARCH DIRECTORATE	2
ATTN: RR-AM	1
RR-C	1
RR-ME	1
RR-PS	1
TECHNICAL LIBRARY	5
TECHNICAL PUBLICATIONS & EDITING BRANCH	2
DIRECTOR, OPERATIONS DIRECTORATE	1
DIRECTOR, PROCUREMENT DIRECTORATE	1
DIRECTOR, PRODUCT ASSURANCE DIRECTORATE	1
PATENT ADVISORS	1

EXTERNAL DISTRIBUTION LIST

December 1976

1 copy to each

OFC OF THE DIR. OF DEFENSE R&E
ATTN: ASST DIRECTOR MATERIALS
THE PENTAGON
WASHINGTON, D.C. 20315

CDR
US ARMY TANK-AUTMV COMD
ATTN: AMDTA-UL
AMSTA-RKM MAT LAB
WARREN, MICHIGAN 48090

CDR
PICATINNY ARSENAL
ATTN: SARPA-TS-S
SARPA-VP3 (PLASTICS
TECH EVAL CEN)
DOVER, NJ 07801

CDR
FRANKFORD ARSENAL
ATTN: SARFA
PHILADELPHIA, PA 19137

DIRECTOR
US ARMY BALLISTIC RSCH LABS
ATTN: AMXBR-LB
ABERDEEN PROVING GROUND
MARYLAND 21005

CDR
US ARMY RSCH OFC (DURHAM)
BOX CM, DUKE STATION
ATTN: RDRD-IPL
DURHAM, NC 27706

CDR
WEST POINT MIL ACADEMY
ATTN: CHMN, MECH ENGR DEPT
WEST POINT, NY 10996

CDR
HQ, US ARMY AVN SCH
ATTN: OFC OF THE LIBRARIAN
FT RUCKER, ALABAMA 36362

CDR
US ARMY ARMT COMD
ATTN: AMSAR-PPW-IR
AMSAR-RD
AMSAR-RDG
ROCK ISLAND, IL 61201

CDR
US ARMY ARMT COMD
FLD SVC DIV
ARMCOM ARMT SYS OFC
ATTN: AMSAR-ASF
ROCK ISLAND, IL 61201

CDR
US ARMY ELCT COMD
FT MONMOUTH, NJ 07703

CDR
REDSTONE ARSENAL
ATTN: AMSMI-RRS
AMSMI-RSM
ALABAMA 35809

CDR
ROCK ISLAND ARSENAL
ATTN: SARRI-RDD
ROCK ISLAND, IL 61202

CDR
US ARMY FGN SCIENCE & TECH CEN
ATTN: AMXST-SD
220 7TH STREET N.E.
CHARLOTTESVILLE, VA 22901

DIRECTOR
US ARMY PDN EQ. AGENCY
ATTN: AMXPE-MT
ROCK ISLAND, IL 61201

EXTERNAL DISTRIBUTION LIST (Cont)

1 copy to each

CDR
US NAVAL WPNS LAB
CHIEF, MAT SCIENCE DIV
ATTN: MR. D. MALYEVAC
DAHLGREN, VA 22448

DIRECTOR
NAVAL RSCH LAB
ATTN: DIR. MECH DIV
WASHINGTON, D.C. 20375

DIRECTOR
NAVAL RSCH LAB
CODE 26-27 (DOCU LIB.)
WASHINGTON, D.C. 20375

NASA SCIENTIFIC & TECH INFO FAC
PO BOX 8757, ATTN: ACQ BR
BALTIMORE/WASHINGTON INTL AIRPORT
MARYLAND 21240

DEFENSE METALS INFO CEN
BATTELLE INSTITUTE
505 KING AVE
COLUMBUS, OHIO 43201

MANUEL E. PRADO / G. STISSER
LAWRENCE LIVERMORE LAB
PO BOX 808
LIVERMORE, CA 94550

DR. ROBERT QUATTRONE
CHIEF, MAT BR
US ARMY R&S GROUP, EUR
BOX 65, FPO N.Y. 09510

2 copies to each

CDR
US ARMY MOB EQUIP RSCH & DEV COMD
ATTN: TECH DOCU CEN
FT BELVOIR, VA 22060

CDR
US ARMY MAT RSCH AGCY
ATTN: AMXMR - TECH INFO CEN
WATERTOWN, MASS 02172

CDR
WRIGHT-PATTERSON AFB
ATTN: AFML/MXA
OHIO 45433

CDR
REDSTONE ARSENAL
ATTN: DOCU & TECH INFO BR
ALABAMA 35809

12 copies

CDR
DEFENSE DOCU CEN
ATTN: DDC-TCA
CAMERON STATION
ALEXANDRIA, VA 22314

NOTE: PLEASE NOTIFY CDR, WATERVLIET ARSENAL, ATTN: SARWV-RT-TP, WATERVLIET, N.Y. 12189, IF ANY CHANGE IS REQUIRED TO THE ABOVE.